JOURNAL OF VIROLOGY, Nov. 2005, p. 14088–14094 Vol. 79, No. 22
0022-538X/05/$08.00+0 doi:10.1128/JVI.79.22.14088–14094.2005

Crystal Structure of Enteric Adenovirus Serotype 41 Short Fiber Head

Elena Seiradake and Stephen Cusack*

EMBL Grenoble Outstation, 38042 Grenoble Cedex 9, France

Received 12 July 2005/Accepted 24 August 2005

Human enteric adenoviruses of species F contain two fibers in the same virion, a long fiber which binds to coxsackievirus and adenovirus receptor (CAR) and a short fiber of unknown function. We have determined the high-resolution crystal structure of the short fiber head of human adenovirus serotype 41 (Ad41). The short fiber head has the characteristic fold of other known fiber heads but has three unusual features. First, it has much shorter loops between the beta-strands. Second, one of the usually well-ordered beta-strands on the distal face of the fiber head is highly disordered and this same region is sensitive to digestion with pepsin, an enzyme occurring naturally in the intestinal tract, the physiological environment of Ad41. Third, the AB loop has a deletion giving it a distinct conformation incompatible with CAR binding.

Adenoviruses are nonenveloped double-stranded DNA viruses, infecting all vertebrate classes. They display a characteristic, icosahedral capsid architecture in which 240 subunits of the trimeric hexon protein form the facets and 12 copies of the penton, comprising the pentameric penton base protein and the externally projecting trimeric fiber, form the vertices. The ~50 serotypes known to infect humans are divided into 6 subgroups (A to F) and cause a range of usually mild respiratory, ocular, or enteric disease. In addition to its importance as a pathogen, adenovirus has for some time been developed as an efficient gene transfer vector for applications in vaccination, cancer treatment and gene therapy.

Virus tropism and the mechanism of cell entry are of considerable current interest, both to improve fundamental understanding of viral pathogenicity and to permit rational engineering and targeting of adenovirus vectors. Mainly based on studies with subgroup C viruses, notably adenovirus type 2 (Ad2), adenovirus cell entry has been characterized as a two-step process. First the fiber head domain binds to a primary cellular receptor, such as the coxsackie and adenovirus receptor (CAR) in the case of subgroups A and C to F (4, 32, 36), or CD46 in the case of some subgroup D and most subgroup B serotypes (17, 30, 38). In a second step, the penton base binds to cellular integrins, triggering internalization via endocytosis (37).

Integrin binding is mediated by an RGD motif in the penton base that is conserved in all human adenovirus serotypes except members of subgroup F, the enteric adenoviruses Ad40 and Ad41 (1). These viruses do not use integrins for cell entry (1) and may use an alternative mechanism for facilitating endocytosis. Strikingly, and in contrast to all other human adenovirus species, enteric adenoviruses also possess two different fiber proteins, both of which are found in each virion in approximately equal numbers (8, 15, 22). There is a long fiber, which has been shown to bind CAR (29) and, additionally, a short fiber that does not bind CAR (29), and is of unknown function. It is possible that these two unique properties of enteric adenoviruses, namely the absence of an RGD motif in the penton base and the unusual presence of a second fiber are related to the special ability of these viruses to infect cells in the human gastric system. Further characteristics of enteric adenoviruses are the relatively high isoelectric point of their structural proteins, increased viability after exposure to an acidic environment (as found in parts of the gastric tract), and their ability to bind certain lipids commonly found in gastric mucosa, especially after exposure to low pH (14).

In order to give further insight into the function of the enteric adenovirus short fiber we have determined the high resolution crystal structure of the Ad41 short fiber head, at both pH 5 and pH 8. These structures reveal an unexpected poorly ordered region on the top of the molecule that we show to contain a specific cleavage site for the digestive enzyme pepsin.

MATERIALS AND METHODS

Expression, purification, and crystallization of Ad41 short fiber head. A vector derived from pBAT4 encoding residues 199 to 387 of Ad41 short fiber head (accession number X17016) was kindly provided by J. Chroboczek and used as a template for smaller Ad41 short fiber head constructs. A DNA fragment coding for residues 215 to 387, and including an Nco1 and an EcoR1 site, was produced by PCR and cloned into a pETDuet-1 MCS1 (Novagen) cloning site together with a C-terminal 6 × His tag (-SGHHHHHH).

The primers used were 5′ AATAATCCATGGGACGCATTGCTATTAGTA ATAGC 3′ (forward primer) and 5′ AATAATGAATTCTTAGTGATGGTGA TGGTGATGGCCGCTTTGTTCAGTTATGTAGCA 3′ (reverse primer). The construct was transformed into *Escherichia coli* BL21 codon plus cells (Stratagen) for expression and these grown in shakers at 37°C to an optical density at 600 nm of 0.6. Protein expression was induced with 0.4 mM IPTG and the temperature lowered to 20°C. After 16 h postinduction the cells were harvested by centrifugation (15 min at 5,000 × g), resuspended in lysis buffer (20 mM Tris-HCl pH 7.9, 500 mM NaCl, 20 mM imidazole, complete EDTA-free protease inhibitor cocktail), and lysed by sonication. The cell lysate was centrifuged for 30 min at 25,000 × g and the supernatant containing soluble protein loaded on a Ni-nitrilotriacetic acid column (QIAGEN). Protein bound to the resin was washed with wash buffer 1 (20 mM Tris-HCl pH 7.9, 1 M NaCl, 20 mM imidazole) and wash buffer 2 (20 mM Tris-HCl pH 7.9, 500 mM NaCl, 80 mM imidazole) and eluted with elution buffer (20 mM Tris-HCl pH 7.9, 500 mM NaCl, 200 mM imidazole).

The eluted protein was concentrated and loaded onto a Superdex 200 column (Pharmacia). During this step the buffer was changed to crystallization buffer (500 mM NaCl, 20 mM Tris pH 7.9). Peak fractions were pooled and concentrated to a final protein concentration of 18 mg/ml. Crystals were obtained in

* Corresponding author. Mailing address: EMBL Grenoble Outstation, 6 rue Jules Horowitz, BP181, 38042 Grenoble Cedex 9, France. Phone: 33-4-76-20-72-38. Fax: 33-4-76-20-71-99. E-mail: cusack@embl-grenoble.fr.

TABLE 1. Data collection and refinement

Parameter	Crystal at pH 5	Crystal transferred to pH 8
Space group	$I\,2_13$	$I\,2_13$
Cell dimensions	a = b = c = 103.8 Å, α = β = γ = 90°	a = b = c = 103.7 Å, α = β = γ = 90°
Resolution range (Å)	36.0–1.5	32.8–1.15
Completeness (last shell)	0.89 (0.89)	0.95 (0.94)
Rsym (last shell)	0.06 (0.19)	0.09 (0.41)
R-factor (last shell)	0.16 (0.22)	0.12 (0.18)
R-free (last shell)	0.16 (0.26)	0.13 (0.18)
No. of atoms (nonhydrogen)	1,454	1,543
No. of reflections used in refinement	25,236	58,983
Fraction of reflections used for R-free calculation	0.05	0.05
Solvent content	46.5	46.7
Mean B-value	14.4	13.32
Ramachandran plot of nonglycine and nonproline residues		
Most favorable regions	117 (85%)	112 (87.5%)
Additional allowed regions	21 (15%)	16 (12.5%)
Generously allowed and disallowed regions	None	None
RMS deviations from ideal values		
Bond distance (Å)	0.008	0.009
Angles	1.2°	1.5°

hanging drops containing 1 μl protein solution (18 mg/ml) with 1 μl crystallization solution 1 (0.25 M sodium phosphate monobasic, 20% polyethylene glycol 3350, pH 5) after one day at 4°C. For the initial data collection single crystals were frozen in a cryoprotectant solution (15% Peg3350, 0.25 M sodium phosphate monobasic, 20% glycerol). For a second data set, single crystals were transferred with 9 intermediate steps to crystallization solution 2 (0.25 M disodium hydrogen phosphate, 20% polyethylene glycol 3350, pH 8). The 9 intermediate solutions had the following ratios of crystallization solution 1 to 2 (9:1, 8:2, 7:3, 6:4, 5:5, 4:6, 3:7, 2:8, and 1:9). The crystals were soaked for 20 min in crystallization solution 2 and frozen in a cryoprotectant solution (0.125 M disodium hydrogen phosphate, 15% polyethylene glycol 3350, 20% glycerol).

Data collection and processing and molecular replacement. Initial diffraction data (crystal at pH 5) was collected to 1.5 Å resolution at the European Synchrotron Radiation Facility (beam line Id14, EH3) using an MAR charge-coupled device detector. Data was integrated with MOSFLM (24) and scaled with SCALA (7). Molecular replacement was performed with MOLREP (33) using the Ad2 fiber head as a model (34). 9 N-terminal residues (388 to 396) were deleted from the input model as they were not part of the core structure. The first solution had an R-factor of 55.5% and a correlation factor of 20.6%, while the second best solution had an R-factor of 60.9% and a correlation factor of 10.5%.

The Ad41 fiber head model including water molecules were automatically built with ARP/wARP (28) using the top solution from the molecular replacement. A region comprising residues 335 to 346, as well as the N-terminal residues 215 to 229 were not automatically built, as they were relatively disordered. Xtalview (25) and COOT (12) were used for calculation of density maps or for the visualization of maps generated with REFMAC (26). Residues 335 to 346 and residue 229 were built manually with these programs. The model passed through several rounds of refinement including anisotropic B-factor refinement and TLS refinement using REFMAC. PROCHECK (23) was used to check the geometry of the model. Crystallographic details and results are summarized in Table 1.

A second data set (crystal at pH 8) was collected to 1.15 Å resolution at the European Synchrotron Radiation Facility (beam line Id14, EH2) using an ADSC Quantum4 detector. Data was integrated and scaled using XDS (21) and further processed with programs of the CCP4 suite (7). Molecular replacement was performed with MOLREP using the previously solved structure of Ad41 short fiber head at 1.5 Å resolution as a model. The first solution had an R-factor of 37.9% and a correlation factor of 59.5%, while the second best solution had an R-factor of 55.5% and a correlation factor of 20.1%. Residues 335 to 346 were removed as no density could be assigned to this part of the model. Waters were added with COOT and the structure refined in REFMAC including anisotropic B-factor refinement, TLS refinement and addition of hydrogen atoms. PROCHECK was used to check the geometry of the model. Crystallographic details and results are summarized in Table 1.

Models of adenovirus fiber heads were superposed with COOT and cartoon representations generated using PYMOL (10). GRASP (27) was used to calculate and display electrostatic surface potentials of fiber head models. Surface areas were calculated using AREAIMOL of the CCP4 package. Residues involved in trimer formation were identified using DIMPLOT (35). For the structure-based sequence alignment, structures were superposed using SARF (2), edited manually using SEAVIEW (18) and visualized with ESPript (19).

Pepsin digestion. The Ad41 short fiber head was expressed purified as described above. An Ad37 fiber head was expressed and purified as described (6). Purified protein solutions were concentrated to 1 mg/ml and dialyzed against digestion buffer (20 mM citric acid pH 3, 500 mM NaCl) at 4°C overnight. Porcine pepsin (P7012, lyophilized powder, 2,500 to 3,500 units/mg, Sigma) was diluted to a stock solution of 100 mg/ml with distilled pure water, as recommended by the seller. For digestion experiments, pepsin was mixed with protein in digestion buffer at a ratio of 1:2 (wt/wt) at room temperature. Samples were taken every 5, 10, 20, 30, 60, and 120 min and the reaction was stopped by adding 2x sample loading buffer (100 mM Tris-HCl pH 6.8, 4% sodium dodecyl sulfate, 20% glycerol, 0.04% bromophenol blue, 10% beta-mercaptoethanol) and boiling for 5 min, or by bringing the pH to 7.5 with buffered Tris and loading onto a Superdex 75 column (Pharmacia). Samples were run both on 13.5% Tris-Tricine-polyacrylamide gels and on 17% sodium dodecyl sulfate/polyacrylamide gels.

RESULTS

Expression and crystallization of Ad41 short fiber head (residues 215 to 387). Ad41 short fiber head was expressed in *E. coli* originally with an N-terminal His tag and a tobacco etch virus protease cleavage site. However this construct tended to form small soluble aggregates that typically contained three trimers as observed by negative stain electron microscopy (data not shown). Furthermore attempts to remove the His tag by tobacco etch virus NIa protease digestion were unsuccessful. An alternative construct with a C-terminal His tag was successfully crystallized without tag removal. Crystals were obtained at pH 5, space group $I2_13$, and the structure solved by molecular replacement using as model the Ad2 fiber head structure (PDB entry 1qhv). The structure was refined to 1.5 Å with an R-factor and R-free of 0.16 (PDB entry 2bzu). To assess the possible effect of pH on the structure, a crystal obtained under the same crystallization conditions was sequentially transferred to solutions of increasing pH and maintained for 20 min at pH 8 before freezing. Data collected on this crystal extended to 1.15 Å (PDB entry 2bzv). Crystallographic details are given in Table 1.

Structure of Ad41 short fiber head is unique, although it displays the typical cloverleaf like architecture found in adenovirus fibers. All adenovirus fiber heads studied so far, in-

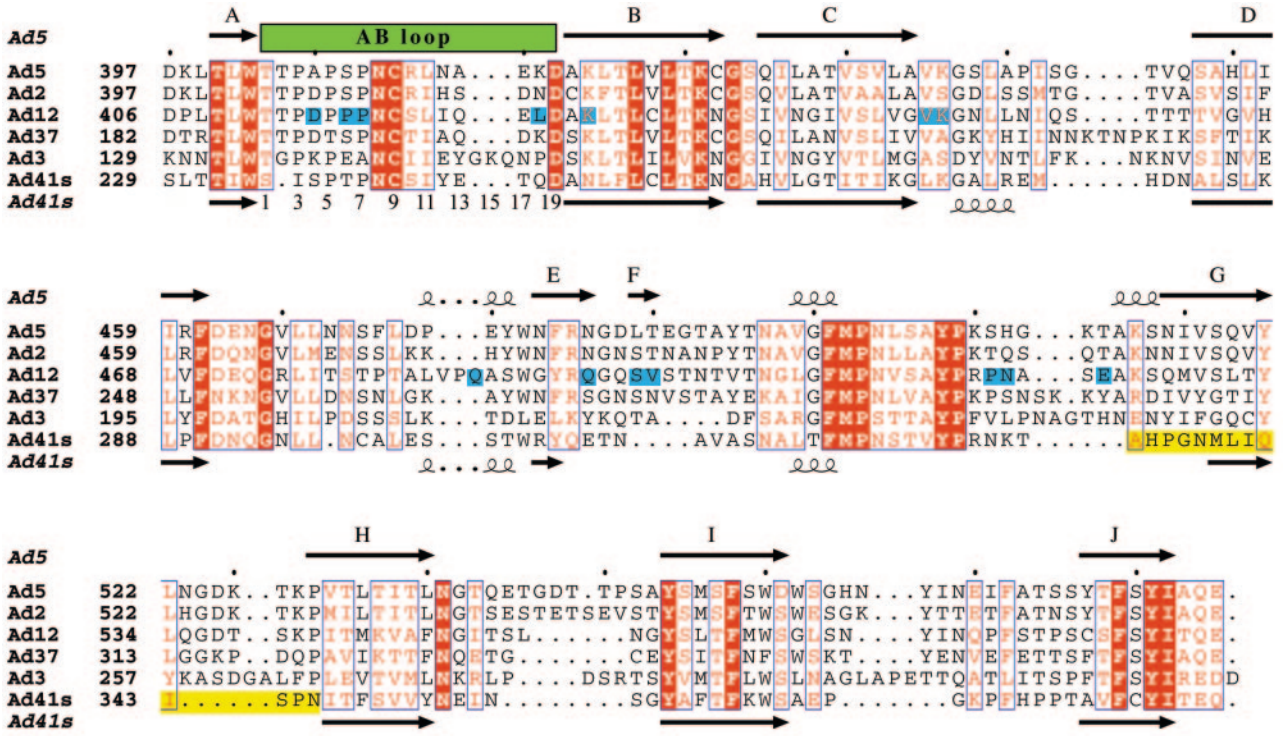

FIG. 1. Structure-based sequence alignment of all adenovirus fiber heads with known crystal structure. Structures were aligned with SARF (2), edited manually with SEAVIEW (18) and visualized with ESPript (19). Red boxes highlight conserved residues. Partially conserved residues are in red. A blue background highlights residues that contact CAR in the structure of Ad12 fiber head complexed with the D1 domain of CAR (20). The AB loop is indicated with a green box over the corresponding sequences, numbers from 1 to 19 have been assigned to residue positions within this loop and are indicated below the corresponding sequences. A yellow background box highlights the disordered region in Ad41.

cluding Ad41 short fiber head, consist of three eight-stranded antiparallel beta-barrels that form a homotrimeric head. Ad41 short fiber head stands out due to two intriguing differences. First, of the otherwise strictly conserved and well-ordered eight β-strands, one, designated strand G (Fig. 1) in other fiber head structures and which is the strand on the top of the molecule closest to the threefold axis (Fig. 2), is severely disordered in Ad41 short fiber head. Residues 335 to 346, which will be referred to as region G, could only be tentatively traced in the structure obtained from crystals at pH 5. B-values are about three times higher in region G than in the rest of the structure, indicating high flexibility. In the 1.15 Å resolution structure at pH 8, region G was completely absent from the electron density, while the rest of the structure does not differ in any significant way from that at pH 5. The integrity of the protein within crystals formed under the same conditions as those used for data collection was checked on SDS page and showed no degradation (Fig. 3) confirming that the poor electron density and high mobility of region G is not due to chain cleavage.

Second, as expected from the sequence, which is about 20 amino acids shorter than in all other known adenovirus fiber head structures, the loops connecting beta-strands are comparably short (Fig. 1). Instead, water-filled spaces are found in between monomers, making the trimer less compact than most other fiber heads (Fig. 2). The percentage of surface per monomer buried upon trimer formation, as well as the number of residues involved in monomer-monomer interaction is lowest among all fiber head structures known (Table 2).

Ad41 short fiber head is cut into distinct fragments by pepsin. In digestion experiments with high concentrations of enteric protease pepsin, Ad41 short fiber head showed less stability compared to Ad37 fiber head, used as a control. Here we present the results obtained from digestion with pepsin (pepsin-fiber head = 1:2 [wt/wt]), which were unambiguously reproduced in all four independent experiments carried out. A number of potential pepsin cleavage sites can be found within the Ad41 short fiber head primary sequence, however digestion at pH 3 resulted in two main fragments after 15 min (Fig. 3). N-terminal sequencing showed that the larger of the two fragments (~14 kDa) includes the N terminus, while the smaller of the two fragments (~6 kDa) comprises a C-terminal fragment starting from residue Ile-341, which is within region G. The size of the intact protein monomer including the His tag is 20.1 kDa.

Western blot analysis with anti-His antibodies confirmed that the smaller fragment still contained the uncleaved His tag at the C terminus, it therefore includes all residues from Ile-341 to the C-terminal end of the Ad41 short fiber head and at least part of the C-terminal His tag. After 2 h of digestion, the big N-terminal fragment is partially cleaved to yield a slightly smaller fragment, while the small C-terminal fragment remains stable. Both large and the small fragment elute together from a Superdex 75 column, at a volume that corresponds to the size of trimeric fiber head (~60 kDa) (Fig. 3). All conditions tested that resulted in fragmentation of Ad41 fiber head did not visibly alter the size of Ad37 fiber head (used as a control) on

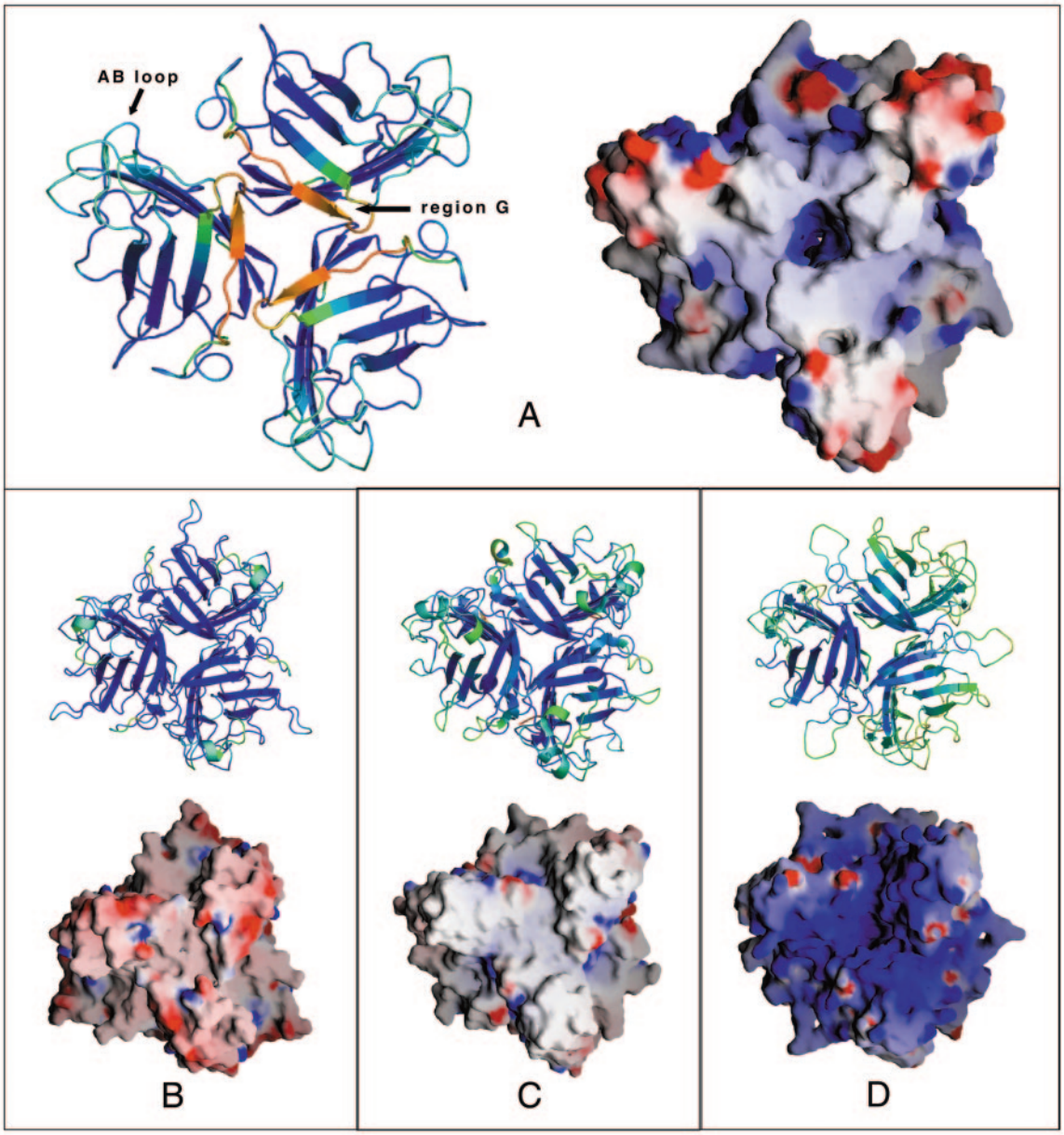

FIG. 2. Comparison of known adenovirus fiber head structures. Cartoon colors are generated by PYMOL (10) according to relative B-values. Blue shows lowest B-values, and red shows highest B-values. The molecular surface and electrostatic surface potential was calculated using GRASP (27). Colors range from red (potential of −10 kT) to blue (+10 kT). (A) Ad41 short fiber head, structure at 1.5 Å resolution, pH 5. (B) Ad2 fiber head (34). (C) Ad12 fiber head (5). (D) Ad37 fiber head (6).

an SDS-PAGE. The Ad37 polypeptide was therefore not digested by the protease under these conditions, at least not at any position distant to either of its termini. Note that adenovirus fiber head migration properties differ depending on the composition of the gel. Ad37 fiber head does not enter Tris-Tricine-polyacrylamide gels very well, and often produces a smear above the expected band. To demonstrate the behavior of the two proteins on a regular 17% SDS/polyacrylamide gel, the same nondigested (T/min 0′) and digested samples (T/min 5′) were loaded again separately. However, the small fragment resulting from pepsin digestion of Ad41 short fiber head is too small to be visualized on this type of gel (Fig. 3).

Structure of the AB loop. A loop between beta-strands A and B, commonly referred to as the AB loop, has been shown to be important for interaction with CAR in CAR-binding adenovirus fibers (5). In Ad41 short fiber this region differs significantly in sequence (there is a single residue deletion) and conformation from CAR-binding fiber heads and this most likely contributes to its inability to bind CAR (Fig. 1, Fig. 4, and Discussion).

DISCUSSION

During the last decade it has become obvious that adenovirus infection does not depend on one single entry pathway, but

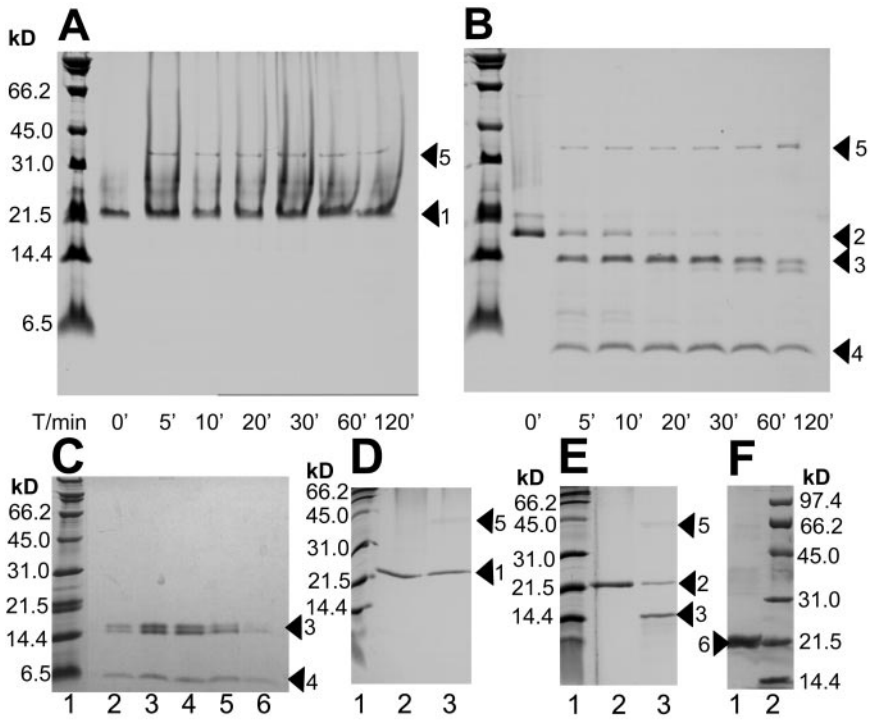

FIG. 3. Effect of pepsin on Ad41 and Ad37 fiber heads. Treatment with pepsin (pepsin-fiber head = 1:2 [wt/wt]) was done at pH 3, room temperature. Samples were taken at 6 different time points and analyzed by SDS PAGE and Coomassie staining on a 13.5% Tris-Tricine-polyacrylamide gel or 17% SDS/polyacrylamide gel. Digestion products of Ad41 fiber head were loaded on a Superdex 75 column (Pharmacia). Lane T/min 0′ represents the respective fiber prior to incubation with pepsin. Sizes corresponding to marker proteins are indicated. (A) Ad37 fiber head visualized on a 13.5% Tris-Tricine-polyacrylamide gel. Arrow 1, full-length protein. Arrow 5, pepsin protease. (B) Ad41 short fiber head visualized on a 13.5% Tris-Tricine-polyacrylamide gel. Arrow 2, full-length protein. Arrow 3, digestion products containing N-terminal residues. Arrow 4, digestion products containing the C terminus from Ile-341. Arrow 5, pepsin protease. (C) Ad41 short fiber head after 2 h digestion with pepsin (fiber head-pepsin = 2:1 [wt/wt]) at 20°C was loaded onto a Superdex 75 column. Peak fractions were visualized on a 13.5% Tris-Tricine-polyacrylamid gel. (Lanes 2 to 6). Arrow 3, digestion products containing N-terminal residues. Arrow 4, digestion products containing the C terminus from Ile-341. (D) Ad37 fiber head visualized on a 17% SDS/polyacrylamide gel. Arrow 1, full-length protein. Arrow 5, pepsin protease. (E) Ad41 short fiber head visualized on a 17% SDS/polyacrylamide gel. Arrow 2, full-length protein. Arrow 3, digestion products containing N-terminal residues. Arrow 5, pepsin protease. Note that the C-terminal fragment is too small to be visualized on this gel. F: Lane 1, arrow 6: Ad41 short fiber head crystals grown at pH 5 after washing, dissolving in SDS sample loading buffer, and visualization on a 15% SDS/polyacrylamide gel.

that alternative pathways must exist (3, 16). Previous studies on subgroup C adenoviruses lead to a cell infection model that involves two steps: an initial step where the fiber head binds to a primary receptor (e.g., CAR) and a second step in which the viral penton bind to cellular integrins via an RGD. Enteric adenoviruses do not use integrins for cell infection and lack an RGD motif on the penton, instead they contain two different fibers, of which the longer one binds to CAR. The short fiber does not bind CAR and its function is not yet known. A previous study has shown that particular physicochemical properties of Ad41 virions adapt it to be stable and able to replicate in the gastrointestinal tract (14). Here we report a study of the atomic structure of the enigmatic Ad41 short fiber aimed at giving insight into possible unique features that might be important in the entry pathway of enteric viruses.

Although Ad41 short fiber head looks superficially similar to other fiber heads its crystal structure reveals some novel features. Most striking is the break with the canonical fold of eight

TABLE 2. Surface of fiber head monomers and trimers

Human adenovirus serotype	Surface area per monomer (Å^2)	Surface area per trimer (Å^2)	Total surface area buried upon trimer formation per trimer (Å^2)	% of surface buried upon trimer formation per monomer	No. of residues per monomer interacting with neighboring monomers
Ad2	10,241	22,066	8,657	28	42
Ad5	8,911	20,800	5,933	22	29
Ad12	8,797	20,250	6,141	23	36
Ad37	9,144	21,340	6,062	22	39
Ad3	9,850	24,297	5,253	18	23[a]
Ad41 (short)	8,312	20,984	3,952	16	22

[a] Mostly hydrophobic.

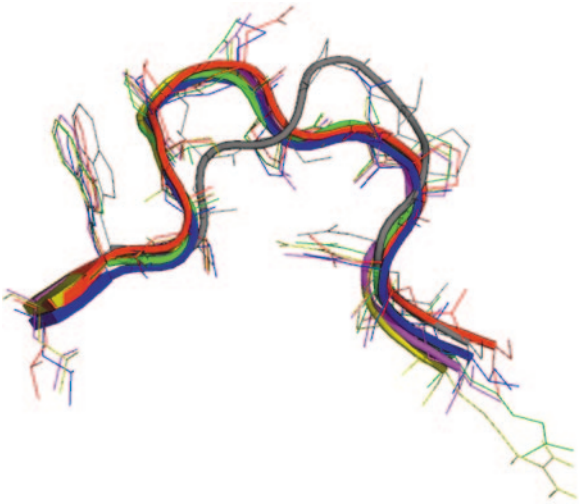

FIG. 4. Conformation of the CAR binding AB loop. Comparative structures of a region implicated in CAR-binding in the AB loop after structural superposition of different adenovirus fiber heads using COOT. Note that the conformation of Ad37 and Ad12 AB loops corresponds to that found in complex with CAR. Red: Ad12 fiber head, green: Ad2 fiber head, blue: Ad3 fiber head, yellow: Ad5 fiber head, magenta: Ad37 fiber head (as found in complex with CAR), gray: Ad41 short fiber head.

well-ordered anti-parallel β-strands per monomer. There is effectively no beta-strand G and instead the corresponding region forms a poorly ordered loop with partial beta-strand-like character at pH 5 (Fig. 2), and no traceable structure at pH 8. Very likely a two-residue motif at the beginning of region G (Pro-336 Gly-337) contributes to the flexibility of the region.

The electrostatic potential distribution on the surface of adenovirus fiber heads varies among serotypes (Fig. 2). The isoelectric point of adenovirus fiber heads crystallized so far ranges from 4.97 (Ad3) to 9.14 (Ad37) and this is reflected in the electrostatic surface. Ad41 short fiber head has a isoelectric point of 6.82, similar to that of respiratory CAR-binding types, such as Ad2 fiber head (pI = 6.25). Distinct basic and acidic regions are visible on the surface of Ad41 short fiber head and it remains to be seen whether these correlate with function. However, the complete Ad41 short fiber protein including the shaft has a pI of 9.13 and the possible implications of this have been discussed previously (14).

The reason Ad41 short fiber head does not bind CAR is probably multifold. Whereas rather few interacting residues are strictly conserved in CAR-binding fibers, an important region is the loop between β-strands A and B, called the AB loop (5). The structure-based sequence alignment (Fig. 1) reveals that the AB loop of Ad41 short fiber head, while containing prolines and small polar residues (serine and threonine), as in CAR binding serotypes, differs in having a single-residue deletion, resulting in a significant change in the conformation of this loop.

Figure 4 shows the three-dimensional conformation of the AB loops of all adenovirus fiber head structures available, after superposition of the entire molecule. Note that the conformation of the Ad37 AB loop corresponds to that found in complex with CAR (Seiradake and Cusack, unpublished results). All AB loop backbone conformations are similar except that of Ad41 short fiber, which is not compatible with CAR binding (e.g., this conformation does not allow the interaction of CAR with the backbone oxygen at position 4 as seen in the Ad12 fiber head-CAR complex). It is interesting that Ad3 fiber head does not bind CAR due to the occurrence of noncomplementary lysine and glutamate residues in the AB loop despite having a compatible backbone conformation (11).

It is intriguing to find that the short fiber of an enteric adenovirus is sensitive to proteolysis with the gastric protease pepsin preferentially in the region G that is different from the canonical adenovirus fiber head architecture. Digestion with digestive tract proteases has been shown to enhance infectivity of some enteric pathogens, such as rotavirus (13). A similar phenomenon cannot be excluded for Ad41. However, digestion with pepsin does not disrupt Ad41 short fiber head trimer formation, as the fragments elute together from a Superdex 75 column (Fig. 3) at the same volume as the nondigested Ad41 short fiber head trimer (results not shown). This observation suggests that a drastic rearrangement of the entire polypeptide chain upon cleavage is unlikely, although region G will clearly be modified. Unfortunately we have not been successful in trying to crystallize the pepsin-cleaved form.

Interestingly, previous experiments (14) had shown that digestion with chymotrypsin also does not affect trimerization of either full-length short or long Ad41 fibers copurified with pentons from infected mammalian cells. In this study however the samples were not analyzed under denaturing conditions, and it is therefore not apparent whether chymotrypsin cut the polypeptide chain or not (14). Clearly, one of the interesting questions for future studies will be whether the cleavage by gastric proteases we find in vitro actually occurs in vivo and if so, what role this might serve.

Considering the function of other fiber head domains and their exposed position at the distal tip of each fiber, it is likely that Ad41 short fiber head plays a major role in enteric adenovirus tropism and cell infection. Solving the structure of the short fiber head of Ad41 to high resolution has helped give insight into how this fiber head differs from other fiber heads of known structure and opens the way for future functional characterization. As Ad41 is particularly well suited for the development of gene transfer vectors to human intestinal epithelial cells (9), this information could be useful in the design of vectors for the treatment of intestinal diseases.

ACKNOWLEDGMENTS

We thank the ESRF for synchrotron facilities and Thibaut Crepin and Chloe Zubieta for assistance at the beamlines. We are grateful to Jadwiga Chroboczek for the gift of the plasmid template and for useful scientific discussions.

Elena Seiradake is supported by an E-STAR fellowship funded by the EU FP6 Marie Curie Host fellowship for Early Stage Research Training under contract number MEST-CT-2004-504640.

REFERENCES

1. **Albinsson, B., and A. H. Kidd.** 1999. Adenovirus type 41 lacks an RGD alpha(v)-integrin binding motif on the penton base and undergoes delayed uptake in A549 cells. Virus Res. **64:**125–136.
2. **Alexandrov, N. N., and D. Fischer.** 1996. Analysis of topological and nontopological structural similarities in the PDB: new examples with old structures. Proteins **25:**354–365.
3. **Bai, M., B. Harfe, and P. Freimuth.** 1993. Mutations that alter an Arg-Gly-Asp (RGD) sequence in the adenovirus type 2 penton base protein abolish

its cell-rounding activity and delay virus reproduction in flat cells. J. Virol. **67:**5198–5205.
4. **Bergelson, J. M., J. A. Cunningham, G. Droguett, E. A. Kurt-Jones, A. Krithivas, J. S. Hong, M. S. Horwitz, R. L. Crowell, and R. W. Finberg.** 1997. Isolation of a common receptor for Coxsackie B viruses and adenoviruses 2 and 5. Science **275:**1320–1323.
5. **Bewley, M. C., K. Springer, Y. B. Zhang, P. Freimuth, and J. M. Flanagan.** 1999. Structural analysis of the mechanism of adenovirus binding to its human cellular receptor, CAR. Science **286:**1579–1583.
6. **Burmeister, W. P., D. Guilligay, S. Cusack, G. Wadell, and N. Arnberg.** 2004. Crystal structure of species D adenovirus fiber knobs and their sialic acid binding sites. J. Virol. **78:**7727–7736.
7. **CCP4 Collaborative Computational Project.** 1994. The CCP4 suite: programs for protein crystallography. Acta Crystallogr. D Biol. Crystallogr. **50:**760–763.
8. **Chroboczek, J., R. W. Ruigrok, and S. Cusack.** 1995. Adenovirus fiber. Curr. Top. Microbiol. Immunol. **199:**163–200.
9. **Croyle, M. A., M. Stone, G. L. Amidon, and B. J. Roessler.** 1998. In vitro and in vivo assessment of adenovirus 41 as a vector for gene delivery to the intestine. Gene Ther. **5:**645–654.
10. **DeLano, W. L.** 2002. The PyMOL molecular graphics system. DeLano Scientific, San Carlos, Calif.
11. **Durmort, C., C. Stehlin, G. Schoehn, A. Mitraki, E. Drouet, S. Cusack, and W. P. Burmeister.** 2001. Structure of the fiber head of Ad3, a non-CAR-binding serotype of adenovirus. Virology **285:**302–312.
12. **Emsley, P., and K. Cowtan.** 2004. Coot: model-building tools for molecular graphics. Acta Crystallogr. D Biol. Crystallogr. **60:**2126–2132.
13. **Estes, M. K., D. Y. Graham, and B. B. Mason.** 1981. Proteolytic enhancement of rotavirus infectivity: molecular mechanisms. J. Virol. **39:**879–888.
14. **Favier, A. L., W. P. Burmeister, and J. Chroboczek.** 2004. Unique physicochemical properties of human enteric Ad41 responsible for its survival and replication in the gastrointestinal tract. Virology **322:**93–104.
15. **Favier, A. L., G. Schoehn, M. Jaquinod, C. Harsi, and J. Chroboczek.** 2002. Structural studies of human enteric adenovirus type 41. Virology **293:**75–85.
16. **Freimuth, P.** 1996. A human cell line selected for resistance to adenovirus infection has reduced levels of the virus receptor. J. Virol. **70:**4081–4085.
17. **Gaggar, A., D. M. Shayakhmetov, and A. Lieber.** 19 October 2003. CD46 is a cellular receptor for group B adenoviruses. Nat. Med. **9:**1408–1412.
18. **Galtier, N., M. Gouy, and C. Gautier.** 1996. SEAVIEW and PHYLO_WIN: two graphic tools for sequence alignment and molecular phylogeny. Comput. Appl. Biosci. **12:**543–548.
19. **Gouet, P., E. Courcelle, D. I. Stuart, and F. Metoz.** 1999. ESPript: analysis of multiple sequence alignments in PostScript. Bioinformatics **15:**305–308.
20. **Howitt, J., M. C. Bewley, V. Graziano, J. M. Flanagan, and P. Freimuth.** 2003. Structural basis for variation in adenovirus affinity for the cellular coxsackievirus and adenovirus receptor. J. Biol. Chem. **278:**26208–26215.
21. **Kabsch, W.** 1988. Evaluation of single-crystal X-ray diffraction data from a position-sensitive detector. J. Appl. Crystallogr. **21:**916–924.
22. **Kidd, A. H., J. Chroboczek, S. Cusack, and R. W. Ruigrok.** 1993. Adenovirus type 40 virions contain two distinct fibers. Virology **192:**73–84.
23. **Laskowski, R. A., M. W. MacArthur, D. S. Moss, and J. M. Thornton.** 1993. PROCHECK: a program to check the stereochemical quality of protein structures. J. Appl. Crystallogr. **26:**283–291.
24. **Leslie, A. G. W.** 1992. Recent changes to the MOSFLM package for processing film and image plate data. Joint CCP4 + ESF-EAMCB Newsl. Protein Crystallogr. 26.
25. **McRee, D. E.** 1999. XtalView/Xfit–A versatile program for manipulating atomic coordinates and electron density. J. Struct. Biol. **125:**156–165.
26. **Murshudov, G. N., A. A. Vagin, A. Lebedev, K. S. Wilson, and E. J. Dodson.** 1999. Efficient anisotropic refinement of macromolecular structures using FFT. Acta Crystallogr. D Biol. Crystallogr. **55:**247–255.
27. **Nicholls, A., K. A. Sharp, and B. Honig.** 1991. Protein folding and association: insights from the interfacial and thermodynamic properties of hydrocarbons. Proteins **11:**281–296.
28. **Perrakis, A., R. Morris, and V. S. Lamzin.** 1999. Automated protein model building combined with iterative structure refinement. Nat. Struct. Biol **6:**458–463.
29. **Roelvink, P. W., A. Lizonova, J. G. Lee, Y. Li, J. M. Bergelson, R. W. Finberg, D. E. Brough, I. Kovesdi, and T. J. Wickham.** 1998. The coxsackievirus-adenovirus receptor protein can function as a cellular attachment protein for adenovirus serotypes from subgroups A, C, D, E, and F. J. Virol. **72:**7909–7915.
30. **Segerman, A., J. P. Atkinson, M. Marttila, V. Dennerquist, G. Wadell, and N. Arnberg.** 2003. Adenovirus type 11 uses CD46 as a cellular receptor. J. Virol. **77:**9183–9191.
31. **Sirena, D., B. Lilienfeld, M. Eisenhut, S. Kalin, K. Boucke, R. R. Beerli, L. Vogt, C. Ruedl, M. F. Bachmann, U. F. Greber, and S. Hemmi.** 2004. The human membrane cofactor CD46 is a receptor for species B adenovirus serotype 3. J. Virol. **78:**4454–4462.
32. **Tomko, R. P., R. Xu, and L. Philipson.** 1997. HCAR and MCAR: the human and mouse cellular receptors for subgroup C adenoviruses and group B coxsackieviruses. Proc. Natl. Acad. Sci. USA **94:**3352–3356.
33. **Vagin, A., and A. Teplyakov.** 2000. An approach to multi-copy search in molecular replacement. Acta Crystallogr. D Biol. Crystallogr. **56:**1622–1624.
34. **van Raaij, M. J., N. Louis, J. Chroboczek, and S. Cusack.** 1999. Structure of the human adenovirus serotype 2 fiber head domain at 1.5 A resolution. Virology **262:**333–343.
35. **Wallace, A. C., R. A. Laskowski, and J. M. Thornton.** 1995. LIGPLOT: a program to generate schematic diagrams of protein-ligand interactions. Protein Eng. **8:**127–134.
36. **Walters, R. W., P. Freimuth, T. O. Moninger, I. Ganske, J. Zabner, and M. J. Welsh.** 2002. Adenovirus fiber disrupts CAR-mediated intercellular adhesion allowing virus escape. Cell **110:**789–799.
37. **Wickham, T. J., P. Mathias, D. A. Cheresh, and G. R. Nemerow.** 1993. Integrins alpha v beta 3 and alpha v beta 5 promote adenovirus internalization but not virus attachment. Cell **73:**309–319.
38. **Wu, E., S. A. Trauger, L. Pache, T. M. Mullen, D. J. von Seggern, G. Siuzdak, and G. R. Nemerow.** 2004. Membrane cofactor protein is a receptor for adenoviruses associated with epidemic keratoconjunctivitis. J. Virol. **78:**3897–3905.
39. **Xia, D., L. J. Henry, R. D. Gerard, and J. Deisenhofer.** 1994. Crystal structure of the receptor-binding domain of adenovirus type 5 fiber protein at 1.7 A resolution. Structure **2:**1259–1270.